

---

# Semantic Equitable Clustering: A Simple, Fast and Effective Strategy for Vision Transformer

---

**Qihang Fan** <sup>1,2</sup>, **Huaibo Huang**<sup>1\*</sup>, **Mingrui Chen**<sup>1,2</sup>, **Ran He**<sup>1,2</sup>

<sup>1</sup>MAIS & CRIPAC, Institute of Automation, Chinese Academy of Sciences, Beijing, China

<sup>2</sup>School of Artificial Intelligence, University of Chinese Academy of Sciences, Beijing, China

fanqihang.159@gmail.com, huaibo.huang@cripac.ia.ac.cn,

charmier2003@gmail.com, rhe@nlpr.ia.ac.cn

## Abstract

The Vision Transformer (ViT) has gained prominence for its superior relational modeling prowess. However, its global attention mechanism's quadratic complexity poses substantial computational burdens. A common remedy spatially groups tokens for self-attention, reducing computational requirements. Nonetheless, this strategy neglects semantic information in tokens, possibly scattering semantically-linked tokens across distinct groups, thus compromising the efficacy of self-attention intended for modeling inter-token dependencies. Motivated by these insights, we introduce a fast and balanced clustering method, named Semantic Equitable Clustering (SEC). SEC clusters tokens based on their global semantic relevance in an efficient, straightforward manner. In contrast to traditional clustering methods requiring multiple iterations, our method achieves token clustering in a single pass. Additionally, SEC regulates the number of tokens per cluster, ensuring a balanced distribution for effective parallel processing on current computational platforms without necessitating further optimization. Capitalizing on SEC, we propose a versatile vision backbone, SecViT. Comprehensive experiments in image classification, object detection, instance segmentation, and semantic segmentation validate to the effectiveness of SecViT. Remarkably, SecViT attains an impressive **84.2%** image classification accuracy with only **27M** parameters and **4.4G** FLOPs, without the need for additional supervision or data. Code will be available at <https://github.com/qhfan/SecViT>.

## 1 Introduction

Since its inception, the Vision Transformer (ViT)[13] has drawn considerable interest from the research community due to its robust modeling prowess. However, the quadratic complexity of Self-Attention leads to significant computational overhead, thus constraining the practicality of ViT. A variety of strategies have been devised to alleviate this computational load, the most prevalent of which involves token grouping, thereby constraining the attention span of each token[36, 12, 53, 48].

Specifically, the Swin-Transformer [36] partitions tokens into multiple small windows, restricting token attention within each window. The CSWin-Transformer [12] adopts a cross-shaped grouping, endowing each token with a global receptive field. MaxViT [48] amalgamates window and grid attention, facilitating intra-window tokens to attend to their counterparts in other windows. However, these methods, solely reliant on spatial positioning, neglect token semantics, potentially restricting the self-attention's capacity to model semantic dependencies. To mitigate this, DGT [35] employs k-means clustering for query grouping, considering the semantic information of tokens for enhanced

---

\* Huaibo Huang is the corresponding author.

feature learning. Nonetheless, the iterative nature of k-means clustering and the potential for uneven token counts per cluster can impact the efficiency of parallel attention operations.

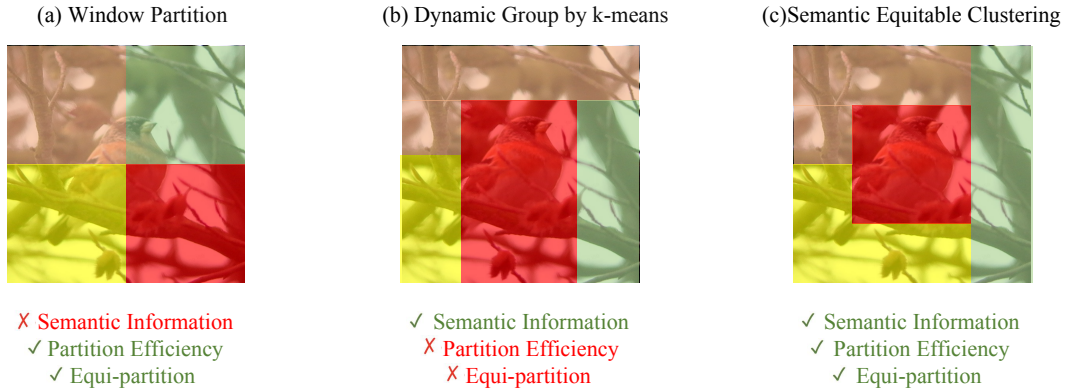


Figure 1: Comparison among Window Partition, Dynamic Group by k-means, and Semantic Equitable Clustering. Our Semantic Equitable Clustering incorporates image semantics while maintaining efficient clustering, eliminating the need for iterative processes such as in k-means. Furthermore, it enables equi-partitioning of tokens, promoting efficient GPU processing without necessitating additional CUDA optimization.

Given these considerations, an optimal token partitioning scheme should efficiently segregate tokens, incorporate semantic information, and efficiently utilize computational resources (e.g., GPU). In response, we introduce a simple, fast and equitable clustering approach named Semantic Equitable Clustering (SEC). SEC segments tokens based on their relevance to global semantic information. Specifically, we employ global pooling to generate a global token encapsulating global semantic information. The similarity between this global token and all other tokens is then computed, reflecting global semantic relevance. Upon obtaining the similarity matrix, tokens (excluding the global token) are sorted by similarity scores, and the tokens with similar scores are grouped into clusters, ensuring uniform token distribution across clusters. As depicted in Fig. 1, SEC comprehensively considers token semantics and completes the clustering process in a single iteration, unlike the multi-iteration k-means. The resulting clusters, containing an equal number of tokens, can be processed in parallel by the GPU efficiently.

Building upon Semantic Equitable Clustering (SEC), we introduce the Semantic Equitable Clustering Vision Transformer (SecViT), a versatile vision backbone that is adaptable to a wide spectrum of downstream tasks. As demonstrated in Fig. 2, SecViT exhibits significant performance improvements compared to previous state-of-the-art (SOTA) models. Impressively, SecViT attains an accuracy of **84.2%** utilizing merely **4.4GFLOPS**, without the need for additional training data or supervision. This superior performance is maintained across different model scales. Furthermore, SecViT proves its proficiency in downstream tasks, including but not limited to, object detection, instance segmentation, and semantic segmentation. For example, SecViT-B achieves **55.1AP<sup>b</sup>** and **47.6AP<sup>m</sup>** with just **111M** Parameters. All above results demonstrate the effectiveness of the proposed SEC.

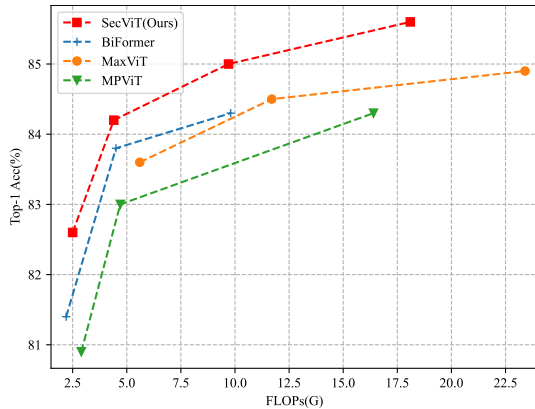


Figure 2: Top-1 accuracy v.s. FLOPs on ImageNet-1K of resent SOTA models. SecViT outperforms all the counterparts in all settings.

## 2 Related works

**Vision Transformer.** The Vision Transformer (ViT) [13] is considered a powerful visual architecture due to its excellent visual modeling capabilities. Many works have improved the Vision Transformer, including enhancing its training efficiency and reducing its computational cost [36, 12, 47, 26, 62]. DeiT uses distillation loss and incorporates extensive data augmentation methods into the ViT training process. This increases the model’s data utilization efficiency, allowing it to train an effective ViT with less data. Hierarchical structures represented by PVT [51, 52, 45, 16, 54] reduce the number of tokens in global attention by downsampling the keys and values (KV), thereby keeping the computational cost of global attention within an acceptable range. In addition to using downsampling to reduce the number of tokens, some methods directly prune tokens based on their importance, retaining important tokens while discarding or merging unimportant ones [15, 42]. This reduces the number of tokens and subsequently lowers the computational cost of the model. Another highly representative approach is to group all tokens such that each token can only attend to tokens within its own group [36, 12, 62, 11, 35]. This method also significantly reduces the computational cost of self-attention.

**Grouping-Based Vision Transformer.** Most grouping-based attention mechanisms perform grouping based on spatial structure [36, 12, 48, 11, 35]. Specifically, the Swin-Transformer [36] divides all tokens into equally sized windows based on their spatial positions, where each token can only attend to tokens within its own window. This significantly reduces the model’s computational cost. In contrast, CSWin [12] divides tokens into a crisscrossing structure, which also reduces the model’s computational cost. In addition to dividing tokens into small windows along the spatial dimension, DaViT [11] also splits channels into multiple groups along the channel dimension. Unlike the above methods that only consider positional information for grouping, DGT [35] takes semantic information into account by using k-means clustering to group the queries.

## 3 Method

### 3.1 Overall Architecture

The overall architecture of SecViT is shown in Fig. 3(a). For each input image  $x \in \mathbb{R}^{3 \times H \times W}$ , we first process it by a patch embedding to downsample it. Then we obtain the tokens with a shape of  $C_1 \times \frac{H}{4} \times \frac{W}{4}$ . Similar to previous work [36, 51, 12], we adopt a hierarchical structure to process tokens. Our model consists of four stages with downsampling factors of  $\frac{1}{4}$ ,  $\frac{1}{8}$ ,  $\frac{1}{16}$ , and  $\frac{1}{32}$ , respectively. This structural design facilitates downstream tasks, such as object detection, in constructing feature pyramids.

A SecViT block is composed of three modules: Conditional Positional Encoding (CPE) [7], Semantic Equitable Clustering based Self-Attention (SECA), and classical Feed-Forward Network (FFN) [49]. A complete SecViT block can be represented by Eq. 1:

$$\begin{aligned} X &= \text{CPE}(X_{in}) + X_{in}, \\ Y &= \text{SECA}(\text{LN}(X)) + X, \\ Z &= \text{FFN}(\text{LN}(Y)) + Y. \end{aligned} \tag{1}$$

For each block, the input tensor  $X_{in} \in \mathbb{R}^{C \times H \times W}$  is fed into the CPE to introduce the positional information. Then, The Self-Attention based on the Semantic Equitable Clustering (SEC) is employed to serve as the token mixer. The final FFN is utilized to integrate channel-wise information of tokens.

### 3.2 Semantic Equitable Clustering

As previously mentioned, the design objectives of Semantic Equitable Clustering are threefold: 1) Fully consider the semantic information contained in different tokens during clustering. 2) Unlike k-means and other clustering methods that require multiple iterations, Semantic Equitable Clustering can complete clustering in a single step. 3) Ensure an equal number of tokens in each cluster to facilitate parallel processing on GPUs. In the following paragraphs, we will describe in detail how our Semantic Equitable Clustering achieves these three objectives. And the whole process is illustrated in the Fig. 3(c).

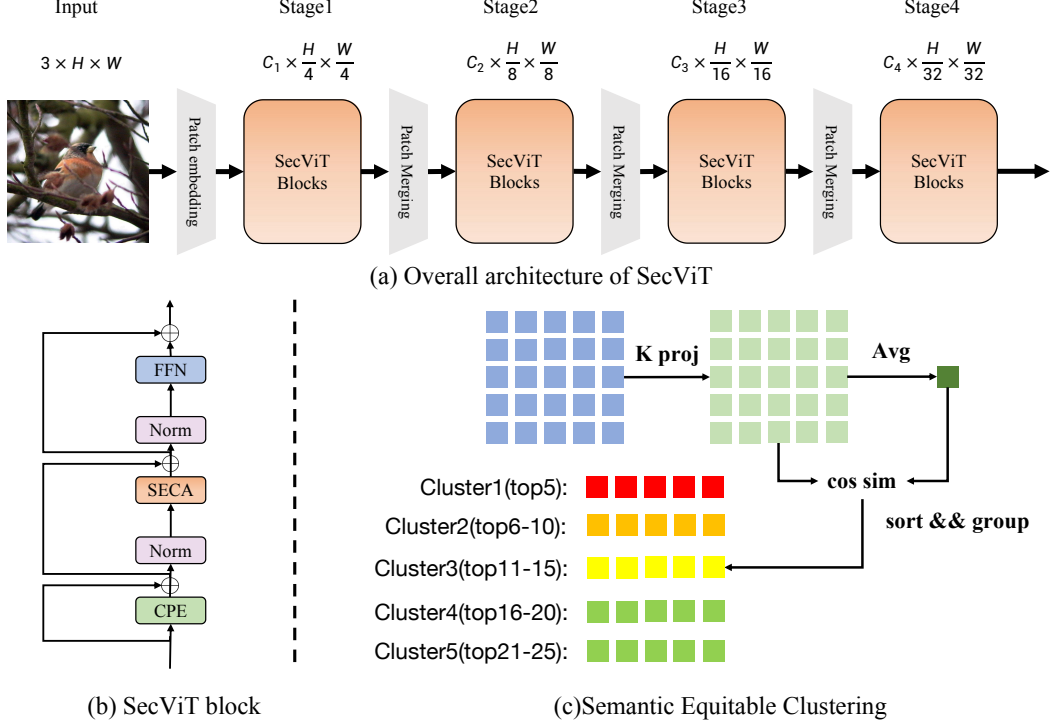


Figure 3: (a) The overall architecture of our Semantic Equitable Clustering Vision Transformer. (b) The composition of each SecViT block. (c) Illustration of our Semantic Equitable Clustering. SEC determines the clustering rules for tokens by calculating the cosine similarity between all tokens and the global token.

**Single Clustering Center Related to Semantics.** K-means is relatively complex for two reasons. **First**, it has multiple cluster centers, and each token needs to calculate its distance to each cluster center to determine its cluster membership. **Second**, the determination of each cluster center in K-means is not precise and requires multiple iterations to accurately establish the cluster centers.

To address these two issues, we first discard the use of multiple cluster centers and instead calculate the distance between each token and a single center. Based on each token’s distance to this center, we divide the tokens into different intervals. Then, to ensure that our chosen center contains the most comprehensive semantic information, we directly use the result of average pooling of all tokens as the center token. This is because, in most vision foundation models, the output of the average pool is assumed to contain the richest semantic information and is thus used for classification [36, 12, 7, 14].

ToMe [2] indicates that the  $K$  contains the richest information from each token. Therefore, we choose the  $K$  as the basis for clustering. Specifically, the process for determining the cluster center is shown in Eq. 2:

$$Q = W_Q X, K = W_K X, V = W_V X, k_c = \text{Avg}(K). \quad (2)$$

Where  $W_K$  is a learnable matrix.  $k_c$  is the determined cluster center.  $X$  is the set of input tokens.

**Distance Metric Suitable for ViT.** Unlike the Euclidean distance calculation used in the K-means algorithm for computing the distance between tokens, during the actual computation of Self-Attention, similarity between query and key is computed through dot product. To better adapt to the characteristics of Self-Attention, we also measure the distance between tokens using a method similar to dot product. Specifically, we calculate the cosine similarity between the cluster center and each token, and then sort the tokens according to the magnitude of the computed results. The specific

process is shown in Eq. 3:

$$\begin{aligned} sim &= \frac{K \cdot k_c}{\|K\| \cdot \|k_c\|}, \\ idx &= \text{argsort}(sim), \\ Q^* &= Q[idx], K^* = K[idx], V^* = V[idx]. \end{aligned} \quad (3)$$

Where  $sim$  is the similarity matrix between  $K$  and  $k_c$ , the  $\text{argsort}(sim)$  returns the indices of  $sim$  sorted in descending order.  $Q^*, K^*, V^*$  are  $Q, K, V$  rearranged according to  $\text{argsort}(sim)$ .

**Equally Partition Tokens based on Distance.** The obtained  $Q^*, K^*,$  and  $V^*$  from the previous step have been sorted based on their distances to the cluster center. At this point, we directly group them, so tokens with similar distances to the cluster center are classified into the same cluster. This allows us to directly control an equal number of tokens in each cluster. This process can be clearly illustrated in Fig. 3(c) and denoted as follows:

$$Q_c = Q_{c \times N_c:(c+1)N_c}^*, K_c = K_{c \times N_c:(c+1)N_c}^*, K_c = K_{c \times N_c:(c+1)N_c}^*. \quad (4)$$

where  $N_c$  is the basic token number of each cluster for equal partition and  $c$  is the index of the cluster

Based on the above steps, we have completed the clustering process that captures semantic information in the image with minimal sorting cost. Moreover, compared to K-means, we have achieved equi-partitioning of each cluster. After clustering is completed, we apply standard Self-Attention to the tokens within each cluster (SECA), thereby completing the interaction of information between tokens:

$$Y_c = \text{Attn}(Q_c, K_c, V_c). \quad (5)$$

After the completion of SECA, to further enhance the model’s ability to capture local information, we employ a local context enhancement module to model local information, where LCE [62, 12] is a simple depth-wise convolution:

$$X = \text{SECA}(X) + \text{LCE}(W_V X), \quad (6)$$

## 4 Experiments

We conducted experiments on a wide range of vision tasks, including image classification on ImageNet-1k [10], object detection and instance segmentation on COCO [33], and semantic segmentation on ADE20K [61]. All models can be trained with 8 A100 80G GPUs.

### 4.1 ImageNet Classification

**Settings.** We train our models from scratch on ImageNet-1k [10]. For a fair comparison, we follow the training strategy in DeiT [47], with classification loss serving as the only supervision. The maximum rates for increasing stochastic depth [23] are set to 0.1, 0.15, 0.4, and 0.5 for SecViT-T, SecViT-S, SecViT-B, and SecViT-L, respectively.

**Comparison with SOTA.** We compare our SecViT with numerous state-of-the-art models, the results are shown in Tab.1. SecViT consistently outperforms preceding models across all scales. Notably, SecViT-S attains a Top1-accuracy of **84.2%** with a mere **15M** parameters and **2.5G** FLOPs. For larger models, SecViT-L achieves a Top1-accuracy of **85.6%** with **96M** parameters and **18.1G** FLOPs.

**Strict Comparison with baselines.** We select two baselines: a general-purpose backbone, Swin-Transformer [36], and a efficiency-oriented backbone, FasterViT [19] to make a comparison with our SecViT. In the comparison models (SEC-Swin and SEC-FasterViT), we merely substitute the attention mechanism in the original Swin-Transformer and FasterViT with our Semantic Equitable Clustering based Self-Attention and without introducing any other modules (such as CPE, Conv Stem, etc.). As shown in Tab. 2, the simple replacement of the attention mechanism yields significant advantages in both performance and efficiency. Specifically, SEC-Swin achieves or even surpasses a **2.0%** improvement over Swin in Tiny and Small model sizes. Meanwhile, SEC-FasterViT attains higher accuracy than FasterViT while utilizing fewer parameters.

Cost	Model	Parmas (M)	FLOPs (G)	Top1-acc (%)	Cost	Model	Parmas (M)	FLOPs (G)	Top1-acc (%)
tiny model ~2.5G	PVTv2-b1 [52]	13	2.1	78.7	base model ~9.0G	Swin-S [36]	50	8.7	83.0
	QuadTree-B-b1 [46]	14	2.3	80.0		ConvNeXt-S [37]	50	8.7	83.1
	RegionViT-T [5]	14	2.4	80.4		CrossFormer-B [53]	52	9.2	83.4
	MPViT-XS [28]	11	2.9	80.9		NAT-S [18]	51	7.8	83.7
	VAN-B1 [17]	14	2.5	81.1		Quadtree-B-b4 [46]	64	11.5	84.0
	BiFormer-T [62]	13	2.2	81.4		ScaleViT-B [58]	81	8.6	84.1
	Conv2Former-N [22]	15	2.2	81.5		MOAT-1 [56]	42	9.1	84.2
	CrossFormer-T [53]	28	2.9	81.5		InternImage-S [50]	50	8.0	84.2
	NAT-M [18]	20	2.7	81.8		DaViT-S [11]	50	8.8	84.2
	FAT-B2 [14]	14	2.0	81.9		BiFormer-B [62]	57	9.8	84.3
	QnA-T [1]	16	2.5	82.0		MViTv2-B [30]	52	10.2	84.4
	GC-ViT-XT [20]	20	2.6	82.0		CMT-B [16]	46	9.3	84.5
	SMT-T [34]	12	2.4	82.2		iFormer-B [45]	48	9.4	84.6
	SecViT-T	15	2.5	<b>82.6</b>		SE-CoTNetD-152 [31]	56	26.5	84.6
	SecViT-B					SecViT-B	55	9.7	<b>85.0</b>
small model ~4.5G	Swin-T [36]	29	4.5	81.3	large model ~18.0G	DeiT-B [47]	86	17.5	81.8
	CrossViT-15 [4]	27	5.8	81.5		Swin-B [36]	88	15.4	83.3
	RVT-S [38]	23	4.7	81.9		LITv2 [40]	87	13.2	83.6
	ConvNeXt-T [37]	29	4.5	82.1		CrossFormer-L [53]	92	16.1	84.0
	Focal-T [57]	29	4.9	82.2		Ortho-L [25]	88	15.4	84.2
	MPViT-S [28]	23	4.7	83.0		CSwin-B [12]	78	15.0	84.2
	SG-Former-S [15]	23	4.8	83.2		SMT-L [34]	81	17.7	84.6
	Ortho-S [25]	24	4.5	83.4		DaViT-B [11]	88	15.5	84.6
	InternImage-T [50]	30	5.0	83.5		SG-Former-B [15]	78	15.6	84.7
	GC-ViT-T [20]	28	4.7	83.5		iFormer-L [45]	87	14.0	84.8
	CMT-S [16]	25	4.0	83.5		CMT-L [16]	75	19.5	84.8
	MaxViT-T [48]	31	5.6	83.6		InterImage-B [50]	97	16.0	84.9
	FAT-B3 [14]	29	4.4	83.6		MaxViT-B [48]	120	23.4	84.9
	SMT-S [34]	20	4.8	83.7		GC-ViT-B [20]	90	14.8	85.0
	BiFormer-S [62]	26	4.5	83.8		SecViT-L	96	18.1	<b>85.6</b>

Table 1: Comparison with the state-of-the-art on ImageNet-1K classification.

Model	Parmas (M)	FLOPs (G)	Throughput (imgs/s)	Top1-acc (%)	Model	Parmas (M)	FLOPs (G)	Throughput (imgs/s)	Top1-acc (%)
Swin-T [36]	29	4.5	1723	81.3	FasterViT-0 [19]	31	3.3	3551	82.1
SEC-Swin-T	29	4.9	1482	<b>83.6(+2.3)</b>	SEC-FasterViT-0	25	3.6	3218	<b>82.6(+0.5)</b>
Swin-S [36]	50	8.8	1062	83.0	FasterViT-1 [19]	53	5.3	2619	83.2
SEC-Swin-S	50	9.3	804	<b>84.8(+1.8)</b>	SEC-FasterViT-1	41	5.6	2486	<b>83.8(+0.6)</b>

Table 2: Strict comparison with the baselines on ImageNet-1K classification. The speed of the models are measured on A100 GPU with the batch size of 64.

## 4.2 Object Detection and Instance Segmentation

**Settings.** We utilize MMDetection [6] to implement Mask-RCNN [21], Cascade Mask R-CNN [3], and RetinaNet [32] to evaluate the performance of the SecViT. For Mask R-CNN and Cascade Mask R-CNN, we follow the commonly used “3 × +MS” setting, and for Mask R-CNN and RetinaNet, we apply the “1×” setting. Following previous works [36, 12, 62], during training, we resize the images such that the shorter side is 800 pixels while keeping the longer side within 1333 pixels.

**Results.** Tab. 3 and Tab. 4 show the results of SecViT with different detection frameworks. The results show that SecViT performs better than its counterparts in all comparisons. For “3 × +MS” schedule, SecViT outperforms the recent InternImage [50] for **+2.2** box AP and **+1.7** mask AP with the framework of Mask R-CNN. Regarding the Cascade Mask R-CNN, SecViT still has very good performance. As for “1×” schedule, SecViT also demonstrate very impressive performance.

## 4.3 Semantic Segmentation

**Settings.** We utilize Semantic FPN [27] and UperNet [55] to validate our SecViT’s performance, implementing these frameworks via MMsegmentation [8]. We follow the PVT’s [51] training settings for Semantic FPN and train the model for 80k iterations. All models use an input resolution of

Backbone	Params		Mask R-CNN 3×+MS						Backbone	Params		Cascade Mask R-CNN 3×+MS					
	(M)	(G)	$AP^b$	$AP_{50}^b$	$AP_{75}^b$	$AP^m$	$AP_{50}^m$	$AP_{75}^m$		(M)	(G)	$AP^b$	$AP_{50}^b$	$AP_{75}^b$	$AP^m$	$AP_{50}^m$	$AP_{75}^m$
Focal-T [57]	49	291	47.2	69.4	51.9	42.7	66.5	45.9	NAT-T [18]	85	737	51.4	70.0	55.9	44.5	67.6	47.9
NAT-T [18]	48	258	47.8	69.0	52.6	42.6	66.0	45.9	GC-ViT-T [20]	85	770	51.6	70.4	56.1	44.6	67.8	48.3
GC-ViT-T [20]	48	291	47.9	70.1	52.8	43.2	67.0	46.7	SMT-S [34]	78	744	51.9	70.5	56.3	44.7	67.8	48.6
MPViT-S [28]	43	268	48.4	70.5	52.6	43.9	67.6	47.5	UniFormer-S [29]	79	747	52.1	71.1	56.6	45.2	68.3	48.9
SMT-S [34]	40	265	49.0	70.1	53.4	43.4	67.3	46.7	Ortho-S [25]	81	755	52.3	71.3	56.8	45.3	68.6	49.2
CSSwin-T [12]	42	279	49.0	70.7	53.7	43.6	67.9	46.6	HorNet-T [43]	80	728	52.4	71.6	56.8	45.6	69.1	49.6
InternImage-T [50]	49	270	49.1	70.4	54.1	43.7	67.3	47.3	CSSwin-T [12]	80	757	52.5	71.5	57.1	45.3	68.8	48.9
SecViT-S	45	259	<b>51.3</b>	<b>72.4</b>	<b>55.9</b>	<b>45.4</b>	<b>69.7</b>	<b>48.8</b>	SecViT-S	83	738	<b>53.9</b>	<b>72.6</b>	<b>58.6</b>	<b>46.7</b>	<b>70.1</b>	<b>51.1</b>
ConvNeXt-S [37]	70	348	47.9	70.0	52.7	42.9	66.9	46.2	Swin-S [36]	107	838	51.9	70.7	56.3	45.0	68.2	48.8
NAT-S [18]	70	330	48.4	69.8	53.2	43.2	66.9	46.4	NAT-S [18]	108	809	51.9	70.4	56.2	44.9	68.2	48.6
Swin-S [36]	69	359	48.5	70.2	53.5	43.3	67.3	46.6	GC-ViT-S [20]	108	866	52.4	71.0	57.1	45.4	68.5	49.3
InternImage-S [50]	69	340	49.7	71.1	54.5	44.5	68.5	47.8	DAT-S [54]	107	857	52.7	71.7	57.2	45.5	69.1	49.3
SMT-B [34]	52	328	49.8	71.0	54.4	44.0	68.0	47.3	CSSwin-S [12]	92	820	53.7	72.2	58.4	46.4	69.6	50.6
CSSwin-S [12]	54	342	50.0	71.3	54.7	44.5	68.4	47.7	UniFormer-B [29]	107	878	53.8	72.8	58.5	46.4	69.9	50.4
SecViT-B	73	368	<b>52.5</b>	<b>73.4</b>	<b>57.6</b>	<b>46.1</b>	<b>70.6</b>	<b>49.8</b>	SecViT-B	111	847	<b>55.1</b>	<b>73.9</b>	<b>59.8</b>	<b>47.6</b>	<b>71.5</b>	<b>51.6</b>

Table 3: Comparison with other backbones using “3×+MS“ schedule on COCO.

Backbone	Params		Mask R-CNN 1×						Backbone	Params		RetinaNet 1×					
	(M)	(G)	$AP^b$	$AP_{50}^b$	$AP_{75}^b$	$AP^m$	$AP_{50}^m$	$AP_{75}^m$		(M)	(G)	$AP^b$	$AP_{50}^b$	$AP_{75}^b$	$AP_S^b$	$AP_M^b$	$AP_L^b$
PVTv2-B1 [52]	33	243	41.8	54.3	45.9	38.8	61.2	41.6	23	225	41.2	61.9	43.9	25.4	44.5	54.3	
FAT-B2 [14]	33	215	45.2	67.9	49.0	41.3	64.6	44.0	23	196	44.0	65.2	47.2	27.5	47.7	58.8	
SecViT-T	34	221	<b>47.7</b>	<b>69.5</b>	<b>52.6</b>	<b>42.9</b>	<b>66.4</b>	<b>46.1</b>	24	202	<b>45.6</b>	<b>66.8</b>	<b>48.9</b>	<b>28.8</b>	<b>49.8</b>	<b>60.7</b>	
Swin-T [36]	48	267	43.7	66.6	47.7	39.8	63.3	42.7	38	248	41.7	63.1	44.3	27.0	45.3	54.7	
CMT-S [16]	45	249	44.6	66.8	48.9	40.7	63.9	43.4	44	231	44.3	65.5	47.5	27.1	48.3	59.1	
MPViT-S [28]	43	268	46.4	68.6	51.2	42.4	65.6	45.7	32	248	45.7	57.3	48.8	28.7	49.7	59.2	
STViT-S [24]	44	252	47.6	70.0	52.3	43.1	66.8	46.5	—	—	—	—	—	—	—	—	
FAT-B3 [14]	49	—	47.6	69.7	52.3	43.1	66.4	46.2	39	—	45.9	66.9	49.5	29.3	50.1	60.9	
BiFormer-S [62]	—	—	47.8	69.8	52.3	43.2	66.8	46.5	—	—	45.9	66.9	49.4	30.2	49.6	61.7	
SecViT-S	45	259	<b>49.7</b>	<b>70.8</b>	<b>54.7</b>	<b>44.2</b>	<b>68.1</b>	<b>48.0</b>	35	240	<b>48.1</b>	<b>69.3</b>	<b>51.8</b>	<b>31.3</b>	<b>53.0</b>	<b>63.6</b>	
Swin-S [36]	69	359	45.7	67.9	50.4	41.1	64.9	44.2	60	339	44.5	66.1	47.4	29.8	48.5	59.1	
ScalableViT-B [58]	95	349	46.8	68.7	51.5	42.5	65.8	45.9	85	330	45.8	67.3	49.2	29.9	49.5	61.0	
InternImage-S [50]	69	340	47.8	69.8	52.8	43.3	67.1	46.7	—	—	—	—	—	—	—	—	
CSSwin-S [12]	54	342	47.9	70.1	52.6	43.2	67.1	46.2	—	—	—	—	—	—	—	—	
STViT-B [24]	70	359	49.7	71.7	54.7	44.8	68.9	48.7	—	—	—	—	—	—	—	—	
SecViT-B	73	368	<b>51.2</b>	<b>72.7</b>	<b>56.4</b>	<b>45.4</b>	<b>69.7</b>	<b>49.0</b>	63	349	<b>48.9</b>	<b>70.2</b>	<b>52.7</b>	<b>32.0</b>	<b>53.6</b>	<b>64.6</b>	
Swin-B [36]	107	496	46.9	69.2	51.6	42.3	66.0	45.5	98	477	45.0	66.4	48.3	28.4	49.1	60.6	
Focal-B [57]	110	533	47.8	70.2	52.5	43.2	67.3	46.5	101	514	46.3	68.0	49.8	31.7	50.4	60.8	
MPViT-B [28]	95	503	48.2	70.0	52.9	43.5	67.1	46.8	85	482	47.0	68.4	50.8	29.4	51.3	61.5	
CSSwin-B [12]	97	526	48.7	70.4	53.9	43.9	67.8	47.3	—	—	—	—	—	—	—	—	
InternImage-B [50]	115	501	48.8	70.9	54.0	44.0	67.8	47.4	—	—	—	—	—	—	—	—	
SecViT-L	115	546	<b>51.9</b>	<b>73.4</b>	<b>57.0</b>	<b>46.1</b>	<b>70.4</b>	<b>49.6</b>	105	527	<b>49.9</b>	<b>71.2</b>	<b>53.7</b>	<b>33.0</b>	<b>54.5</b>	<b>66.1</b>	

Table 4: Comparison to other backbones using “1×“ schedule on COCO.

512 × 512, and during testing, the image’s shorter side is resized to 512 pixels. Different from FPN, the UperNet is trained for 160K iterations and follows Swin’s [36] settings. We employ the AdamW optimizer with a weight decay of 0.01 and a 1500 iteration warm-up.

**Results.** The results of semantic segmentation can be found in the Tab. 5. All the FLOPs are measured with the input resolution of 512 × 2048, except the group of the SecViT-T, which are measured with the input resolution of 512 × 512. SecViT achieves the best performance in all settings. Specifically, with the framework of Semantic FPN, our SecViT-S outperforms FAT-B3 for **+0.6** mIoU. And SecViT-S surpasses CSWin-S by a large margin (**+1.5** mIoU). For the framework of Upernet, SecViT-S surpasses the recent SMT-S by **+1.4** mIoU. SecViT-B and SecViT-L also surpass all their counterparts.

#### 4.4 Ablation Study

**Comparison with Swin-Transformer.** As mentioned earlier, based on the Swin-T architecture, we directly replaced WSA/SWSA with our SECA. As shown in Tab. 6, this resulted in a significant performance improvement (classification accuracy increased by 2.3%).

Semantic FPN			
Backbone	Params(M)	FLOPs(G)	mIoU(%)
PVTv2-B1 [52]	18	34	42.5
FAT-B2 [14]	17	32	45.4
EdgeViT-S [39]	17	32	45.9
SecViT-T	18	34	<b>47.2</b>
DAT-T [54]	32	198	42.6
CSWin-T [12]	26	202	48.2
Shuted-S [44]	26	183	48.2
FAT-B3 [14]	33	179	48.9
SecViT-S	29	177	<b>49.5</b>
DAT-S [54]	53	320	46.1
RegionViT-B+ [5]	77	459	47.5
UniFormer-B [29]	54	350	47.7
CSWin-S [12]	39	271	49.2
SecViT-B	57	288	<b>50.7</b>
DAT-B [54]	92	481	47.0
CrossFormer-L [53]	95	497	48.7
CSWin-B [12]	81	464	49.9
SecViT-L	99	471	<b>52.0</b>

UperNet			
Backbone	Params(M)	FLOPs(G)	mIoU(%)
DAT-T [54]	60	957	45.5
NAT-T [18]	58	934	47.1
InternImage-T [50]	59	944	47.9
MPViT-S [28]	52	943	48.3
SMT-S [34]	50	935	49.2
SecViT-S	56	933	<b>50.6</b>
DAT-S [54]	81	1079	48.3
SMT-B [34]	62	1004	49.6
InternImage-S [50]	80	1017	50.2
MPViT-B [28]	105	1186	50.3
CSWin-S [12]	65	1027	50.4
SecViT-B	84	1046	<b>52.0</b>
Swin-B [36]	121	1188	48.1
GC ViT-B [20]	125	1348	49.2
DAT-B [54]	121	1212	49.4
InternImage-B [50]	128	1185	50.8
CSWin-B [12]	109	1222	51.1
SecViT-L	130	1256	<b>53.6</b>

Table 5: Comparison with the state-of-the-art on ADE20K.

**Comparison with CSWin-Transformer.** As shown in Tab. 6, based on the SecViT-T architecture, we replace SECA with CSWSA from CSwin-Transformer. This leads to a significant drop in classification performance (a decrease of 1.2%). This fully demonstrates the effectiveness of our proposed token clustering method.

**LCE.** LCE is a simple depth-wise convolution module used to further enhance the model’s ability to model local information. We conduct ablation experiments on LCE and find that it contributes to a certain improvement in the model’s performance. The results are shown in Tab. 6. Specifically, it boosts the model’s classification accuracy by **+0.2**.

**CPE.** The CPE proposed in CPVT [7] is a plug-and-play, highly portable positional encoding method, widely adopted by many methods to provide positional information to the model. It consists of a residual block containing only a 3x3 depth-wise convolution.

Ablation results on CPE in Tab. 6 indicate that it offers some performance gains to the model (approximately **+0.2** increase in classification accuracy).

**Conv Stem.** The Conv Stem is utilized in the early stages of the model to extract more refined local features. As indicated by the data in Tab. 6, the Conv Stem enhances the performance of the model to some extent in classification task. Specifically, the Conv Stem improves the classification accuracy by **+0.3**.

**Effect of number of clusters.** In Tab. 7, we validate the impact of different cluster numbers chosen at each of the first three stages of the model on performance. For SecViT-S, we select 32,

Model	Params(M)	FLOPs(G)	Top1-acc(%)
Swin-T	29	4.5	81.3
SEC-Swin-T	29	4.9	<b>83.6(+2.3)</b>
SecViT-T	15	2.5	82.6
SECA→CSWSA [12]	15	2.5	<b>81.4(-1.2)</b>
w/o LCE	15	2.5	82.4
w/o CPE	15	2.5	82.4
w/o Conv Stem	14	2.1	82.3

Table 6: Ablation Study.

num	FLOPs(G)	Top1-acc(%)
64, 16, 4, –	4.3	84.0
64, 16, 2, –	4.3	84.1
64, 8, 2, –	4.3	84.1
32, 8, 2, –	4.4	84.2

Table 7: Effect of number of clusters.

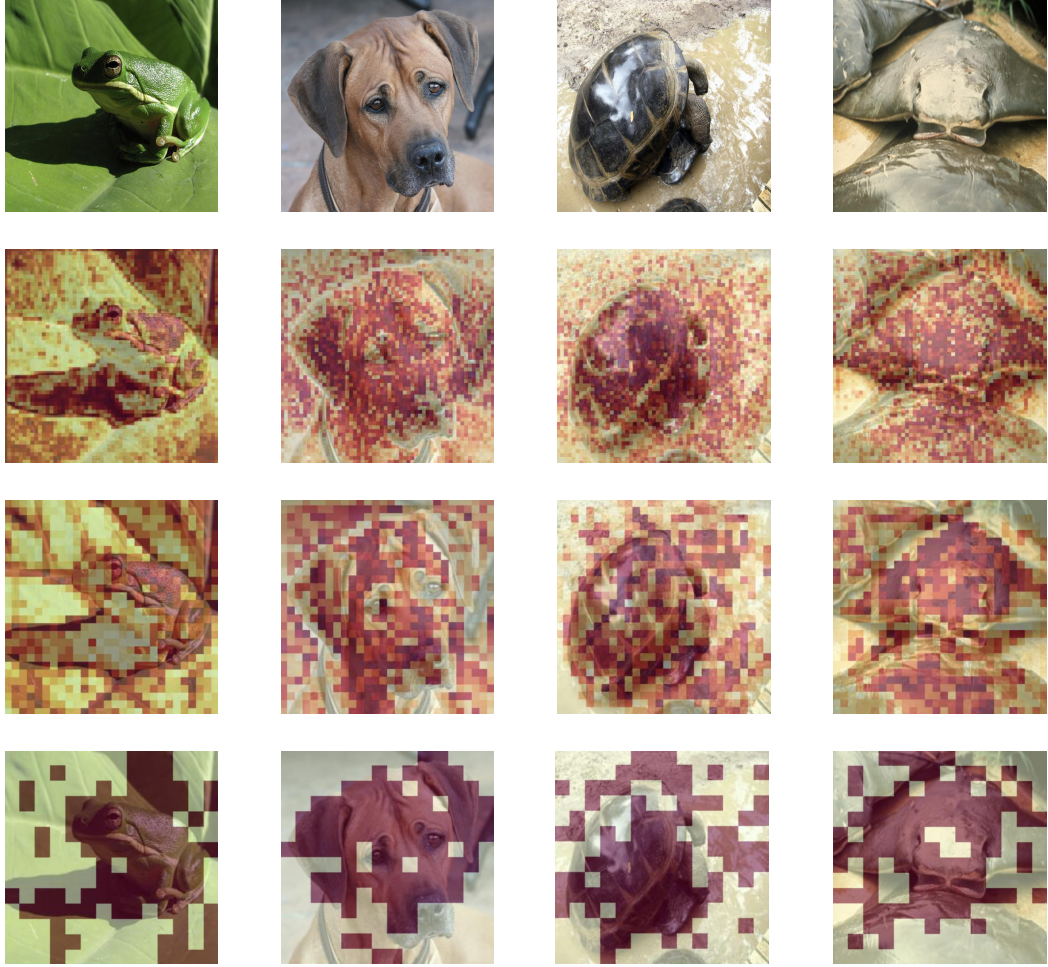


Figure 4: Visualization results for SecViT-B. The first row shows the original images, the second row displays the clustering results of the first stage (32 clusters), the second row displays the clustering results of the second stage (8 clusters), and the third row shows the clustering results of the third stage (2 clusters).

8, and 2 clusters for the first three stages, respectively. This configuration achieves a classification accuracy of 84.2%. As we gradually increase the number of clusters at each stage, the model’s overall computation decreases, with a slight drop in accuracy. This demonstrates the robustness of Semantic Clustering with respect to the number of clusters.

#### 4.5 Visualization of Semantic Clustering

To further understand how our semantic equitable clustering works, we visualized the clustering results of some samples. As shown in Fig. 4, we selected the first, second, and third stages of the pre-trained SecViT-B to observe the clustering results of different tokens. In the figure, patches with the same color belong to the same cluster. It is evident that in the first and second stages, our model tends to capture detailed information, while in the third stage, it tends to capture semantic information.

## 5 Conclusion

We propose a simple and straightforward clustering method for Vision Transformers—Semantic Equitable Clustering (SEC). This method assigns each token to a cluster by calculating the similarity between each token and a global token, then sorting them accordingly. Our clustering method takes

into account the semantic information contained in the tokens, completes the clustering in a single step, and ensures an equal number of tokens in each cluster, facilitating efficient parallel processing on modern GPUs. Based on Semantic Equitable Clustering, we designed SecViT, a versatile vision backbone that achieves impressive results across various vision tasks, including image classification, object detection, instance segmentation, and semantic segmentation.

## References

- [1] Moab Arar, Ariel Shamir, and Amit H. Bermano. Learned queries for efficient local attention. In *CVPR*, 2022.
- [2] Daniel Bolya, Cheng-Yang Fu, Xiaoliang Dai, Peizhao Zhang, Christoph Feichtenhofer, and Judy Hoffman. Token merging: Your ViT but faster. In *ICLR*, 2023.
- [3] Zhaowei Cai and Nuno Vasconcelos. Cascade r-cnn: Delving into high quality object detection. In *CVPR*, 2018.
- [4] Chun-Fu (Richard) Chen, Quanfu Fan, and Rameswar Panda. CrossViT: Cross-Attention Multi-Scale Vision Transformer for Image Classification. In *ICCV*, 2021.
- [5] Chun-Fu (Richard) Chen, Rameswar Panda, and Quanfu Fan. RegionViT: Regional-to-Local Attention for Vision Transformers. In *ICLR*, 2022.
- [6] Kai Chen, Jiaqi Wang, Jiangmiao Pang, et al. MMDetection: Open mmlab detection toolbox and benchmark. *arXiv preprint arXiv:1906.07155*, 2019.
- [7] Xiangxiang Chu, Zhi Tian, Bo Zhang, Xinlong Wang, and Chunhua Shen. Conditional positional encodings for vision transformers. In *ICLR*, 2023.
- [8] MM Segmentation Contributors. Mmsegmentation, an open source semantic segmentation toolbox, 2020.
- [9] Ekin D Cubuk, Barret Zoph, Jonathon Shlens, et al. Randaugment: Practical automated data augmentation with a reduced search space. In *CVPRW*, 2020.
- [10] Jia Deng, Wei Dong, Richard Socher, et al. Imagenet: A large-scale hierarchical image database. In *CVPR*, 2009.
- [11] Mingyu Ding, Bin Xiao, Noel Codella, et al. Davit: Dual attention vision transformers. In *ECCV*, 2022.
- [12] Xiaoyi Dong, Jianmin Bao, Dongdong Chen, et al. Cswin transformer: A general vision transformer backbone with cross-shaped windows. In *CVPR*, 2022.
- [13] Alexey Dosovitskiy, Lucas Beyer, Alexander Kolesnikov, et al. An image is worth 16x16 words: Transformers for image recognition at scale. In *ICLR*, 2021.
- [14] Qihang Fan, Huaibo Huang, Xiaoqiang Zhou, and Ran He. Lightweight vision transformer with bidirectional interaction. In *NeurIPS*, 2023.
- [15] SG-Former: Self guided Transformer with Evolving Token Reallocation. Sucheng ren, xingyi yang, songhua liu, xinchao wang. In *ICCV*, 2023.
- [16] Jianyuan Guo, Kai Han, Han Wu, Chang Xu, Yehui Tang, Chunjing Xu, and Yunhe Wang. Cmt: Convolutional neural networks meet vision transformers. In *CVPR*, 2022.
- [17] Meng-Hao Guo, Cheng-Ze Lu, Zheng-Ning Liu, Ming-Ming Cheng, and Shi-Min Hu. Visual attention network. *arXiv preprint arXiv:2202.09741*, 2022.
- [18] Ali Hassani, Steven Walton, Jiachen Li, Shen Li, and Humphrey Shi. Neighborhood attention transformer. In *CVPR*, 2023.
- [19] Ali Hatamizadeh, Greg Heinrich, Hongxu Yin, Andrew Tao, Jose M Alvarez, Jan Kautz, and Pavlo Molchanov. Fastervit: Fast vision transformers with hierarchical attention. In *ICLR*, 2024.
- [20] Ali Hatamizadeh, Hongxu Yin, Greg Heinrich, Jan Kautz, and Pavlo Molchanov. Global context vision transformers. In *ICML*, 2023.
- [21] Kaiming He, Georgia Gkioxari, Piotr Dollár, and Ross B. Girshick. Mask r-cnn. In *ICCV*, 2017.
- [22] Qibin Hou, Cheng-Ze Lu, Ming-Ming Cheng, and Jiashi Feng. Conv2former: A simple transformer-style convnet for visual recognition. *arXiv preprint arXiv:2211.11943*, 2022.
- [23] Gao Huang, Yu Sun, and Zhuang Liu. Deep networks with stochastic depth. In *ECCV*, 2016.
- [24] Huaibo Huang, Xiaoqiang Zhou, Jie Cao, Ran He, and Tieniu Tan. Vision transformer with super token sampling. In *CVPR*, 2023.
- [25] Huaibo Huang, Xiaoqiang Zhou, and Ran He. Orthogonal transformer: An efficient vision transformer backbone with token orthogonalization. In *NeurIPS*, 2022.
- [26] Zi-Hang Jiang, Qibin Hou, Li Yuan, Daquan Zhou, Yujun Shi, Xiaojie Jin, Anran Wang, and Jiashi Feng. All tokens matter: Token labeling for training better vision transformers. In *NeurIPS*, 2021.
- [27] Alexander Kirillov, Ross Girshick, Kaiming He, and Piotr Dollár. Panoptic feature pyramid networks. In *CVPR*, 2019.
- [28] Youngwan Lee, Jonghee Kim, Jeffrey Willette, and Sung Ju Hwang. Mpvit: Multi-path vision transformer for dense prediction. In *CVPR*, 2022.
- [29] Kunchang Li, Yali Wang, Peng Gao, Guanglu Song, Yu Liu, Hongsheng Li, and Yu Qiao. Uniformer: Unified transformer for efficient spatiotemporal representation learning, 2022.
- [30] Yanghao Li, Chao-Yuan Wu, Haoqi Fan, Karttikeya Mangalam, Bo Xiong, Jitendra Malik, and Christoph Feichtenhofer. Mvitv2: Improved multiscale vision transformers for classification and detection. In *CVPR*, 2022.
- [31] Yehao Li, Ting Yao, Yingwei Pan, and Tao Mei. Contextual transformer networks for visual recognition. *TPAMI*, 2022.

[32] Tsung-Yi Lin, Priya Goyal, Ross B. Girshick, and Kaiming He andPiotr Dollár. Focal loss for dense object detection. In *ICCV*, 2017.

[33] Tsung-Yi Lin, Michael Maire, Serge Belongie, et al. Microsoft coco: Common objects in context. In *ECCV*, 2014.

[34] Weifeng Lin, Ziheng Wu, Jiayu Chen, Jun Huang, and Lianwen Jin. Scale-aware modulation meet transformer. In *ICCV*, 2023.

[35] Kai Liu, Tianyi Wu, Cong Liu, and Guodong Guo. Dynamic group transformer: A general vision transformer backbone with dynamic group attention. In *IJCAI*, 2022.

[36] Ze Liu, Yutong Lin, Yue Cao, Han Hu, Yixuan Wei, Zheng Zhang, Stephen Lin, and Baining Guo. Swin transformer: Hierarchical vision transformer using shifted windows. In *ICCV*, 2021.

[37] Zhuang Liu, Hanzi Mao, Chao-Yuan Wu, et al. A convnet for the 2020s. In *CVPR*, 2022.

[38] Xiaofeng Mao, Gege Qi, Yuefeng Chen, Xiaodan Li, Ranjie Duan, Shaokai Ye, Yuan He, and Hui Xue. Towards robust vision transformer. In *CVPR*, 2022.

[39] Junting Pan, Adrian Bulat, Fuwen Tan, et al. Edgevits: Competing light-weight cnns on mobile devices with vision transformers. In *ECCV*, 2022.

[40] Zizheng Pan, Jianfei Cai, and Bohan Zhuang. Fast vision transformers with hilo attention. In *NeurIPS*, 2022.

[41] Boris T Polyak and Anatoli B Juditsky. Acceleration of stochastic approximation by averaging. *arXiv preprint arXiv:1906.07155*, 2019.

[42] Yongming Rao, Wenliang Zhao, Benlin Liu, Jiwen Lu, Jie Zhou, and Cho-Jui Hsieh. Dynamicvit: Efficient vision transformers with dynamic token sparsification. In *NeurIPS*, 2021.

[43] Yongming Rao, Wenliang Zhao, Yansong Tang, Jie Zhou, Ser-Lam Lim, and Jiwen Lu. Hornet: Efficient high-order spatial interactions with recursive gated convolutions. In *NeurIPS*, 2022.

[44] Sucheng Ren, Daquan Zhou, Shengfeng He, Jiashi Feng, and Xinchao Wang. Shunted self-attention via multi-scale token aggregation. In *CVPR*, 2022.

[45] Chenyang Si, Weihao Yu, Pan Zhou, Yichen Zhou, Xinchao Wang, and Shuicheng YAN. Inception transformer. In *NeurIPS*, 2022.

[46] Shitao Tang, Jiahui Zhang, Siyu Zhu, et al. Quadtree attention for vision transformers. In *ICLR*, 2022.

[47] Hugo Touvron, Matthieu Cord, Matthijs Douze, et al. Training data-efficient image transformers & distillation through attention. In *ICML*, 2021.

[48] Zhengzhong Tu, Hossein Talebi, Han Zhang, Feng Yang, Peyman Milanfar, Alan Bovik, and Yinxiao Li. Maxvit: Multi-axis vision transformer. In *ECCV*, 2022.

[49] Ashish Vaswani, Noam Shazeer, Niki Parmar, et al. Attention is all you need. In *NeurIPS*, 2017.

[50] Wenhui Wang, Jifeng Dai, Zhe Chen, Zhenhang Huang, Zhiqi Li, Xizhou Zhu, Xiaowei Hu, Tong Lu, Lewei Lu, Hongsheng Li, et al. Internimage: Exploring large-scale vision foundation models with deformable convolutions. In *CVPR*, 2023.

[51] Wenhui Wang, Enze Xie, Xiang Li, Deng-Ping Fan, Kaitao Song, Ding Liang, Tong Lu, Ping Luo, and Ling Shao. Pyramid vision transformer: A versatile backbone for dense prediction without convolutions. In *ICCV*, 2021.

[52] Wenhui Wang, Enze Xie, Xiang Li, Deng-Ping Fan, Kaitao Song, Ding Liang, Tong Lu, Ping Luo, and Ling Shao. Pvttv2: Improved baselines with pyramid vision transformer. *Computational Visual Media*, 8(3):1–10, 2022.

[53] Wenxiao Wang, Lu Yao, Long Chen, Binbin Lin, Deng Cai, Xiaofei He, and Wei Liu. Crossformer: A versatile vision transformer hinging on cross-scale attention. In *ICLR*, 2022.

[54] Zhuofan Xia, Xuran Pan, Shiji Song, Li Erran Li, and Gao Huang. Vision transformer with deformable attention. In *CVPR*, 2022.

[55] Tete Xiao, Yingcheng Liu, Bolei Zhou, Yuning Jiang, and Jian Sun. Unified perceptual parsing for scene understanding. In *ECCV*, 2018.

[56] Chenglin Yang, Siyuan Qiao, Qihang Yu, et al. Moat: Alternating mobile convolution and attention brings strong vision models. In *ICLR*, 2023.

[57] Jianwei Yang, Chunyuan Li, Pengchuan Zhang, Xiyang Dai, Bin Xiao, Lu Yuan, and Jianfeng Gao. Focal self-attention for local-global interactions in vision transformers. In *NeurIPS*, 2021.

[58] Rui Yang, Hailong Ma, Jie Wu, Yansong Tang, Xuefeng Xiao, Min Zheng, and Xiu Li. Scalablevit: Rethinking the context-oriented generalization of vision transformer. In *ECCV*, 2022.

[59] Sangdoo Yun, Dongyoon Han, Seong Joon Oh, et al. Cutmix: Regularization strategy to train strong classifiers with localizable features. In *ICCV*, 2019.

[60] Hongyi Zhang, Moustapha Cisse, Yann N Dauphin, et al. mixup: Beyond empirical risk minimization. In *ICLR*, 2018.

[61] Bolei Zhou, Hang Zhao, Xavier Puig, et al. Scene parsing through ade20k dataset. In *CVPR*, 2017.

[62] Lei Zhu, Xinjiang Wang, Zhanghan Ke, Wayne Zhang, and Rynson Lau. Biformer: Vision transformer with bi-level routing attention. In *CVPR*, 2023.

## Supplementary Material

Model	Blocks	Channels	Heads	Ratios	Params(M)	FLOPs(G)
SecViT-T	[2, 2, 9, 2]	[64, 128, 256, 512]	[2, 4, 8, 16]	3	15	2.5
SecViT-S	[3, 4, 18, 4]	[64, 128, 256, 512]	[2, 4, 8, 16]	3	27	4.4
SecViT-B	[4, 8, 26, 8]	[80, 160, 320, 512]	[5, 5, 10, 16]	3	55	9.7
SecViT-L	[4, 8, 26, 8]	[112, 224, 448, 640]	[7, 7, 14, 20]	3	96	18.1
SEC-Swin-T	[2, 2, 6, 2]	[96, 192, 384, 768]	[3, 6, 12, 24]	4	29	4.9
SEC-Swin-S	[2, 2, 18, 2]	[96, 192, 384, 768]	[3, 6, 12, 24]	4	50	9.3
SEC-FasterViT-0	[2, 3, 6, 5]	[64, 128, 256, 512]	[–, –, 8, 16]	4	25	3.6
SEC-FasterViT-1	[1, 3, 8, 5]	[80, 160, 320, 640]	[–, –, 8, 16]	4	41	5.6

Table 8: Detailed Architectures of our models.

## A Architecture Details

SecViT’s architecture details are illustrated in Table 8. In SecViT, we adopt four  $3 \times 3$  convolutions to embed the input image into tokens, batch normalization and GELU are used after each convolution.  $3 \times 3$  convolutions with stride 2 are used between stages to reduce the feature resolution.  $3 \times 3$  DWConvs are adopted in CPE. While  $5 \times 5$  depth-wise convolutions are adopted for LCE.

For SEC-Swin, we adhere to the design principles of the Swin-Transformer [36] without using additional structures such as CPE or Conv Stem.

For SEC-FasterViT, we adhere to the design principles of FasterViT [19]. We use convolutional for fast inference speed in the first two stages of the model and use our Semantic Equitable Clustering based Self-Attention (SECA) in the latter two stages.

For all models, we set the number of clusters in the first three stages to 32, 8, and 2, respectively.

## B Experimental Settings

**ImageNet Image Classification.** We adopt the training strategy proposed in DeiT [47], with the only supervision is cross entropy loss. All of our models are trained from scratch for 300 epochs with the input resolution of  $224 \times 224$ . The AdamW is used with a cosine decay learning rate scheduler and 5 epochs of linear warm-up. The batch-size is set to 1024, respectively. We apply the same data augmentation and regularization used in DeiT [47], including RandAugment [9] (randm9-mstd0.5-inc1) , Mixup [60] (prob = 0.8), CutMix [59] (prob = 1.0), Random Erasing (prob = 0.25), and Exponential Moving Average (EMA) [41]. The maximum rates of increasing stochastic depth [23] are set to 0.1/0.15/0.4/0.5 for SecViT-T/S/B/L.

**COCO Object Detection and Instance Segmentation.** We apply RetinaNet [32], Mask-RCNN [21], and Cascaded Mask R-CNN [3] as the detection frameworks based on the MMDetection [6]. All of our models are trained with “ $1 \times$ ” (12 training epochs) and “ $3 \times +MS$ ” (36 training epochs with multi-scale training) settings. For the “ $1 \times$ ” setting, images are resized to the shorter side of 800 pixels while the longer side is within 1333 pixels. For the “ $3 \times +MS$ ”, multi-scale training strategy is used to randomly resize the shorter side of images between 480 to 800 pixels. For both frameworks, we use the AdamW with the initial learning rate of 1e-4. For RetinaNet, we set the weight decay to 1e-4. While for Mask-RCNN and Cascaded Mask R-CNN, we set it to 5e-2.

**ADE20K Semantic Segmentation.** Based on MM Segmentation [8], we implement UperNet [55] and SemanticFPN [27] to evaluate our models’ performance on semantic segmentation. For UperNet, we follow the previous setting of Swin-Transformer [36] and train the model for 160k iterations with the input size of  $512 \times 512$ . For SemanticFPN, we also use the input resolution of  $512 \times 512$  but train the models for 80k iterations.

## C Limitations and Future Work

While the proposed Semantic Equitable Clustering have demonstrated significant efficiency for clustering tokens and impressive performance on many vision tasks, there are still several limitations that need to be addressed in our future work. First, the computational constraints prevented us from experimenting with larger models and datasets such as ImageNet-21k. Exploring the potential of Semantic Equitable Clustering on large-scale datasets and larger model could provide further insights into its scalability and efficiency. In the future, we will strive to validate the performance of our SecViT on large datasets and with larger models.

## D Broader Impact Statement

The development of the Semantic Equitable Clustering (SEC) has the potential to impact the field of computer vision by offering a efficient and semantic-related approach to group tokens in Vision Transformer. By clustering the tokens, SEC reduces computational load and improves the efficiency of vision models, which could lead to broader applications.

The proposed SecViT is a general vision backbone that can be applied on different vision tasks, e.g., image classification, object detection, instance segmentation, and semantic segmentation. It has no direct negative social impact. Possible malicious uses of SecViT as a general-purpose backbone are beyond the scope of our study to discuss.

## E Code

We provide the code of our Semantic Equitable Clustering base Self-Attention.

```
1  class SECA(nn.Module):
2
3      def __init__(self, embed_dim, num_heads, num_clusters):
4          super().__init__()
5          self.num_clusters = num_clusters
6          self.embed_dim = embed_dim
7          self.num_heads = num_heads
8          self.head_dim = embed_dim // num_heads
9          self.scaling = self.head_dim ** -0.5
10         self.qkv = nn.Conv2d(embed_dim, embed_dim*3, 1, bias=True)
11         self.out_proj = nn.Conv2d(embed_dim, embed_dim, 1, bias=True)
12
13     def sort_sim(self, q: torch.Tensor, k: torch.Tensor):
14         """
15         q: b n (h w) d
16         k: b n (h w) d
17         """
18         cls_token = q.mean(2, keepdim=True) # (b n 1 d)
19         cls_token = F.normalize(cls_token, dim=-1)
20         k = F.normalize(k, dim=-1)
21         cos_sim = cls_token @ k.transpose(-1, -2) # (b n 1 (h w))
22         sort_indices = torch.argsort(cos_sim, dim=-1)
23         return sort_indices.squeeze(2) # (b n (h w))
24
25     def sort_tensor(self, indices: torch.Tensor, target: torch.Tensor):
26         """
27         indices: (b n l)
28         target: (b n l d)
29         """
30         sorted_tensor = torch.gather(target, dim=-2, index=indices.
31             unsqueeze(-1).expand_as(target))
32         return sorted_tensor
33
34     def restore_tensor(self, indices: torch.Tensor, target: torch.
35         Tensor):
```

```

34     """
35     indices: (b n l)
36     target: (b n l d)
37     """
38     restored_tensor = torch.gather(target, dim=-2, index=indices.
39                                     sort(dim=-1).indices.unsqueeze(-1).expand_as(target))
40     return restored_tensor
41
42     def forward(self, x: torch.Tensor):
43         """
44         x: (b c h w)
45         """
46         bsz, _, h, w = x.size()
47         l = h * w
48         assert l % self.num_clusters == 0
49         qkv = self.qkv(x) # (b 3*c h w)
50
51         q, k, v = rearrange(qkv, 'b (m n d) h w -> m b n (h w) d', m
52                             =3, n=self.num_heads)
53         # q, k, v -> b n (h w) d
54         k = k * self.scaling
55
56         if self.num_clusters > 1:
57             indices = self.sort_sim(k, k) # (b n (h w))
58             q = self.sort_tensor(indices, q) # (b n (h w) d)
59             k = self.sort_tensor(indices, k) # (b n (h w) d)
60             v = self.sort_tensor(indices, v) # (b n (h w) d)
61
62             q_l = rearrange(q, 'b n (c l) d -> b n c l d', c=self.
63                             num_clusters)
64             k_l = rearrange(k, 'b n (c l) d -> b n c l d', c=self.
65                             num_clusters)
66             v = rearrange(v, 'b n (c l) d -> b n c l d', c=self.
67                             num_clusters)
68             attn = torch.softmax(q_l @ k_l.transpose(-1, -2), dim=-1)
69             # (b n c l l)
70             v = attn @ v # (b n c l d)
71
72             v = rearrange(v, 'b n c l d -> b n (c l) d')
73             v = self.restore_tensor(indices, v) # (b n (h w) d)
74             v = rearrange(v, 'b n (h w) d -> b (n d) h w', h=h, w=w)
75         else:
76             attn = torch.softmax(q @ k.transpose(-1, -2), dim=-1) # (b
77                             n (h w) (h w))
78             v = attn @ v # (b n (h w) d)
79             v = rearrange(v, 'b n (h w) d -> b (n d) h w', h=h, w=w)
80
81         return self.out_proj(res)

```